Saturation Analysis of a Monolithic Wavelength Converter

Joachim Piprek,[i] John Hutchinson,[a] Jeffrey Henness, Milan Masanovic, and Larry A. Coldren

Electrical and Computer Engineering Department,
University of California, Santa Barbara, CA 93106
[a] Intel Corporation, Portland, OR

ABSTRACT

We investigate the nonlinear response of an InP-based optoelectronic wavelength converter by three-dimensional device simulation including an advanced many-body model for gain and absorption in the InGaAsP quantum wells. The wavelength converter combines a pre-amplified receiver with a post-amplified sampled-grating distributed Bragg reflector tunable laser diode. Good agreement between simulation and measurements is obtained. The nonlinear signal transmission is mainly attributed to quantum well saturation effects in amplifier and photo-detector. Saturation related microscopic physical processes are analyzed in detail.

Keywords: Optoelectronic integrated circuit, wavelength converter, semiconductor optical amplifier, waveguide photo-detector, nonlinear signal transmission, saturation effect, many-body model, three-dimensional numerical simulation

1. INTRODUCTION

Wavelength converters are a novel class of photonic integrated circuits that is crucial for future wavelength-division multiplexing (WDM) fiber-optic communication systems. Their main purpose is to transfer signals from one WDM wavelength to another. Here we report on the simulation and analysis of an optoelectronic InP-based tunable wavelength converter as shown in Fig. 1.

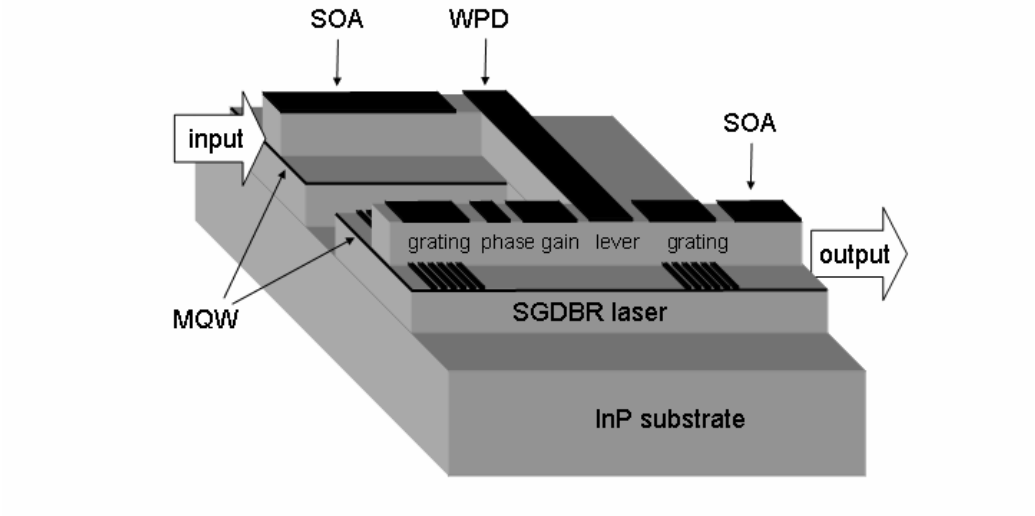

Fig. 1: Schematic view of the InP-based integrated wavelength converter.

[i] Corresponding author, e-mail: piprek@ieee.org

Physics and Applications of Optoelectronic Devices, edited by Joachim Piprek,
Proceedings of SPIE Vol. 5594 (SPIE, Bellingham, WA, 2004)
0277-786X/04/$15 · doi: 10.1117/12.569180

The receiver integrates signal pre-amplification by a semiconductor optical amplifier (SOA) and signal detection by a waveguide photodiode (WPD). The optical signal is converted into an electrical signal that directly modulates a sampled-grating distributed-Bragg-reflector (SGDBR) laser diode which is integrated with a semiconductor optical amplifier (SOA) for signal enhancement.[1] The SGDBR laser can be tuned to emit at any wavelength of the C band.[2]

Layer	Material	Thickness nm	Doping 10^{18} cm^{-3}
p-contact	InGaAs	100	30 (p)
upper cladding	InP	1600	1 (p)
upper cladding	InP	200	0.3 (p)
doping setback	InP	50	-
quantum barrier (8x)	$In_{0.685}Ga_{0.315}As_{0.595}P_{0.405}$	8	-
quantum well (7x)	$In_{0.685}Ga_{0.315}As_{0.864}P_{0.136}$	6.5	-
etch stop	InP	10	-
waveguide	$In_{0.612}Ga_{0.338}As_{0.728}P_{0.272}$	350	0.1 (n)
lower cladding	InP	1400	1 (n)
etch stop / n-contact	InGaAs	100	1 (n)
Buffer	InP	1000	-

Tab. 1 Epitaxial layer sequence of the devices simulated.

The structure of the different components is very similar as all are based on the same epitaxial growth (Tab. 1). An offset multi-quantum-well (MQW) active region is grown on top of the waveguide region. A ridge waveguide structure is etched through the MQW region. Passive device sections are formed by etching off the MQW completely.

2. THEORETICAL MODEL

The three-dimensional (3D) physics-based model takes into account interband gain and absorption in the InGaAsP active region, carrier transport including Fermi statistics and thermionic emission, and optical wave-guiding.[3] However, previous investigations revealed that the free-carrier gain model does not give consistent agreement with experimental results.[4] We therefore combine our 3D simulation with an advanced many-body gain theory[5] which is calibrated to measured photoluminescence spectra of our MQW active region (Fig. 2). Details of the 3D model and of the many-body gain integration are published elsewhere.[6] In the following, we apply this model to the investigation of saturation effects in amplifier and detector.

3. COMPARISON TO MEASUREMENTS

In order to calculate realistic many-body spectra, photoluminescence (PL) measurements on our quantum well structure are used to calibrate the inhomogeneous energy broadening in the model, which represents imperfections of the practical growth process. Fig. 2 shows measured and calculated PL spectra. The emission peak at 1532 nm indicates a slight growth deviation from the intended MQW composition. The PL peak wavelength can be matched in the simulation by adjustment of the MQW composition, maintaining the measured biaxial MQW strain: 0.6% compressive strain in the quantum wells and 0.3% tensile strain in the barriers. This way, we obtain $In_{0.685}Ga_{0.315}As_{0.864}P_{0.136}$ for the quantum well composition and $In_{0.685}Ga_{0.315}As_{0.595}P_{0.405}$ for the barrier composition. The adjustment may also reflect inaccuracies in the calculation of the strained quaternary energy band gap. A full-width half maximum (FWHM) value of 14 meV for the inhomogeneous energy broadening gives good agreement with the experimental PL spectra in Fig. 2, much better than with the free-carrier model.[4]

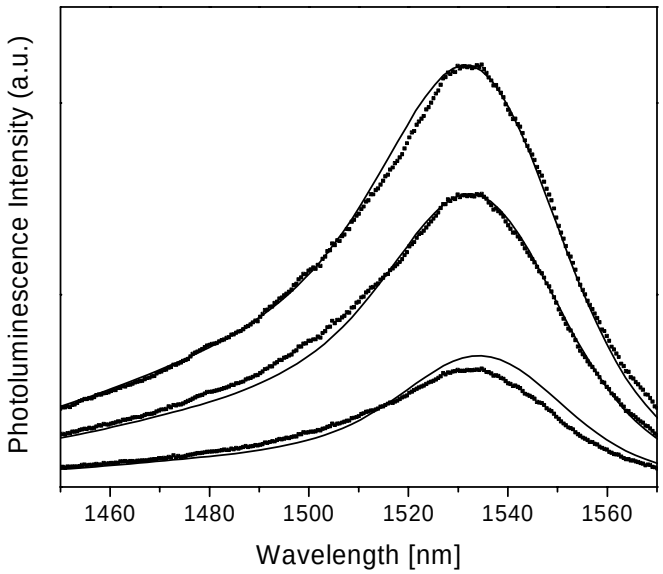

Fig. 2: Photoluminescence spectra of our MQW active region (dots – measured at 1×, 2×, and 3× pump intensity; solid lines - many-body calculations at carrier densities of 3.8, 6.2, and 7.7 $\times 10^{17}$ cm^{-3}).

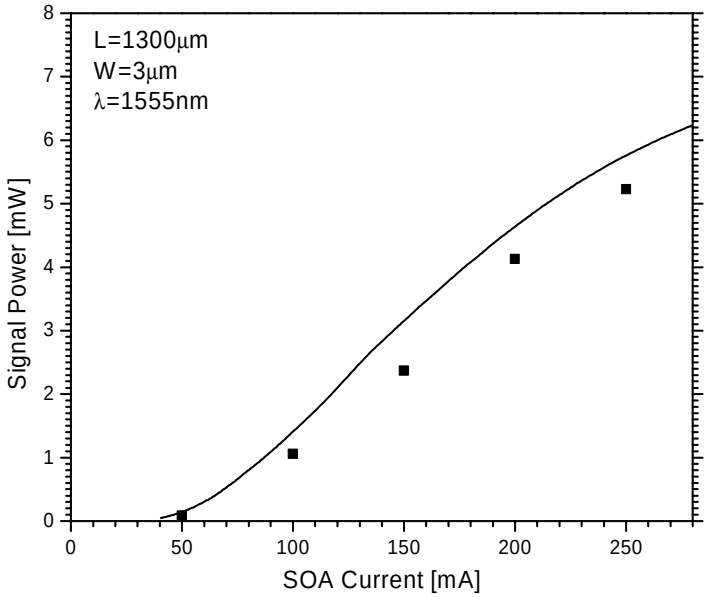

Fig. 3: Comparison of measured (dots) and simulated (lines) amplifier characteristics without ASE (L - amplifier length, W - ridge width, λ - signal wavelength).

Figure 3 shows a comparison between the measured and the simulated signal output power as function of SOA current. We use the same model and parameters as in Ref.[6] without any parameter adjustment. The measurements are performed on individual SOAs with a length of 1300 μm which are not integrated into the wavelength converter. Amplified spontaneous emission (ASE) contributions are subtracted from the experimental output power using a

measurement without input signal. The ASE is expected to be lower when an input signal is present, so the dots in Fig. 3 somewhat underestimate the actual signal power.

4. AMPLIFIER SATURATION

Amplification enhances the optical signal and it compensates for any losses during wavelength conversion. Our semiconductor optical amplifier (SOA) should provide maximum signal gain while maintaining linearity between input and output signal. However, with increasing input power, amplifier saturation results in a sub-linear response which significantly limits the performance of our wavelength converter. In the following, we simulate and analyze the physical mechanisms that cause amplifier saturation. Figure 4 shows the calculated SOA transmission characteristics for three different amplifier currents. Optical coupling losses are neglected. Hardly any performance improvement is achieved by increasing the SOA current from 150 mA to 300 mA, due to the saturation of the material gain with rising quantum well carrier density.[6] Thus, we consider the case with 150 mA current in the following. Transmission nonlinearity becomes obvious at a signal input power of about 1 mW.

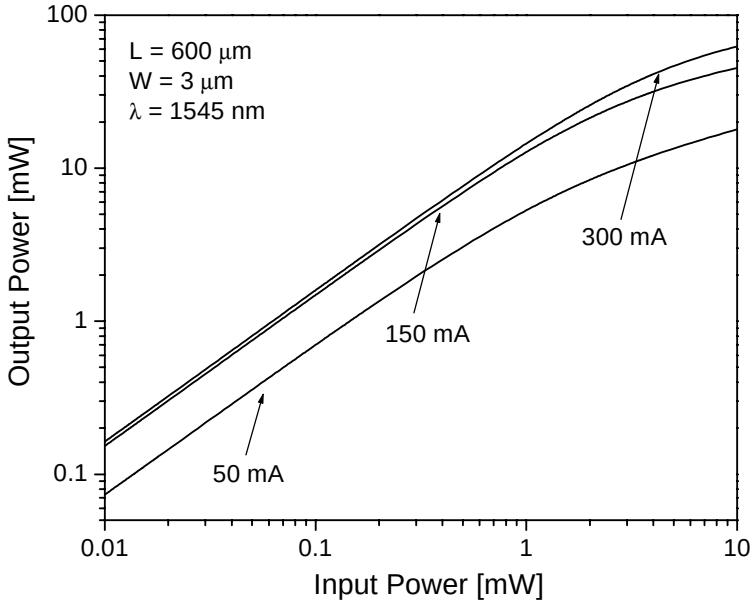

Fig. 4: SOA output power vs. input power with the SOA current as parameter.

Figure 5 plots longitudinal profiles of different physical quantities within the center of the SOA active region. With increasing travel distance of the signal, its optical intensity rises due to stimulated carrier recombination within the quantum wells. The recombination rate is proportional to the local optical intensity, reducing the quantum well carrier density towards the output facet. This leads to the reduction of the local material gain, which limits the amplification of the signal power and causes the sub-linear response in Fig. 4. The transmission characteristic is linear only as long as the internal material properties remain independent of the signal power. The reduction of the quantum well carrier density by enhanced stimulated recombination is the main reason for the nonlinearity of our SOA transmission characteristics.

Figure 6 shows lateral profiles of the same parameters at the output facet. The optical field is laterally confined by the 3μm wide waveguide ridge. The high power of 12 mW at the output facet causes lateral hole burning by enhanced stimulated emission, i.e., the electron density as well as the gain profile exhibit a local minimum in the center of the device where the optical intensity is maximum.

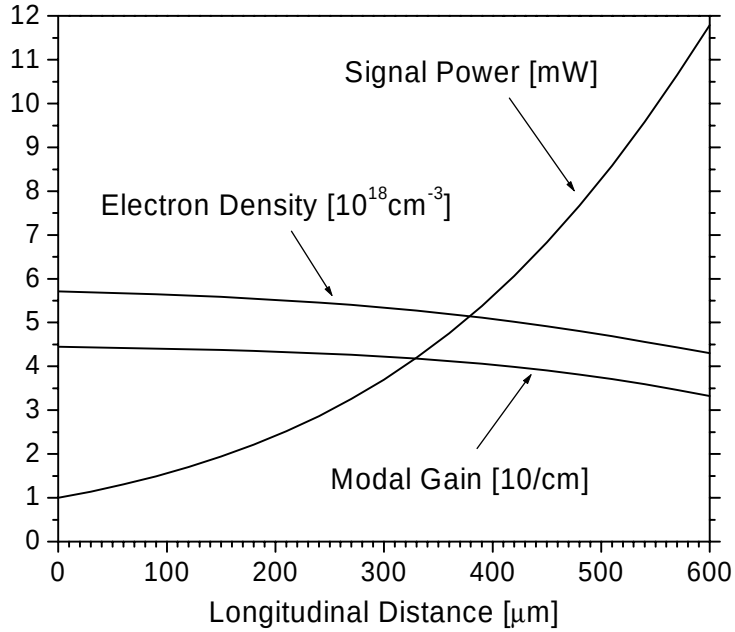

Fig. 5: Longitudinal profiles of internal amplifier parameters in the center quantum well.

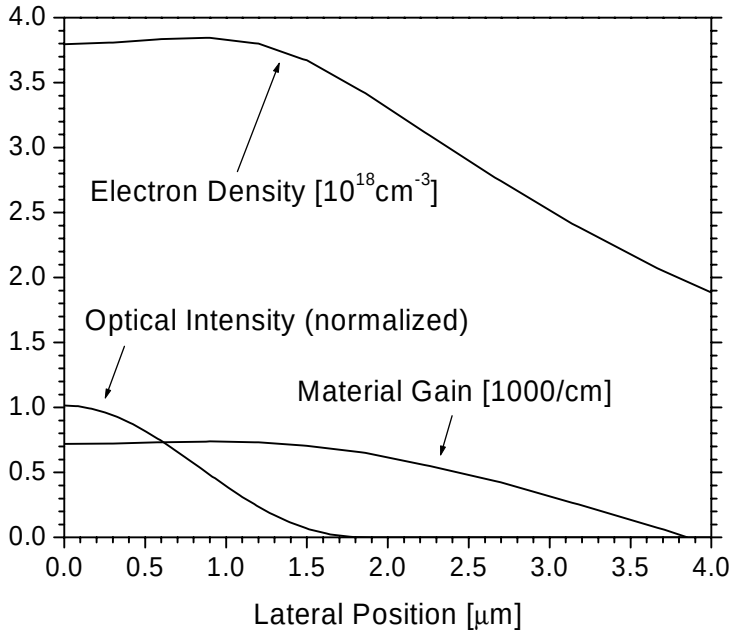

Fig. 6: Lateral profiles of internal amplifier parameters at the output facet.

5. DETECTOR SATURATION

The waveguide photodetector (WPD) is coupled monolithically to the pre-amplifier and we neglect any optical coupling loss. The WPD length is L = 100 μm in our simulation and the ridge width is W = 3 μm. Figure 7 shows the calculated detector response function for two cases with different reverse bias. At lower reverse bias of 1V, the photocurrent is a sublinear function of the input power even for weak signals. At larger reverse bias, the detector response is more linear. We investigate the strongly nonlinear low-voltage case in the following.

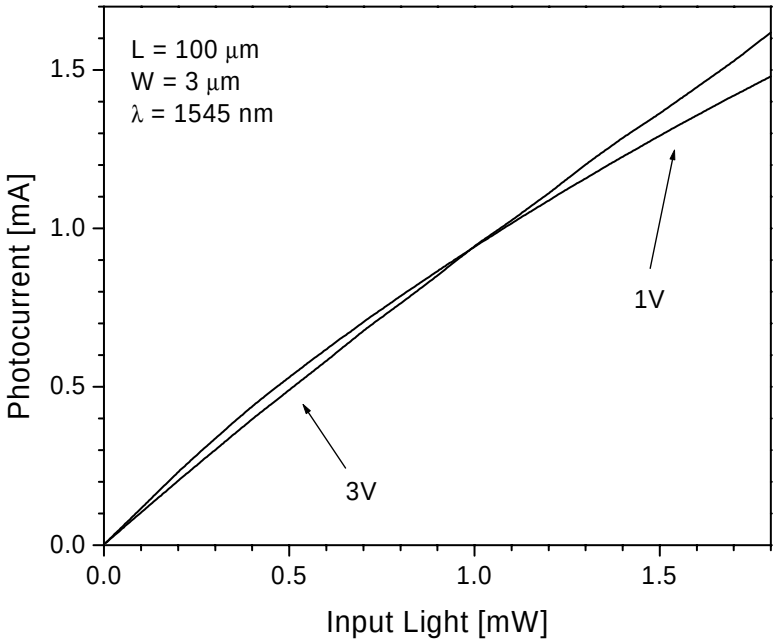

Fig. 7: WPD photocurrent vs. optical input power with the reverse bias as parameter.

Detector saturation effects are mainly related to the accumulation of photo-generated carriers within the quantum wells. Such accumulation depends on the local light power and therefore on the longitudinal position within the detector. Figure 8 shows longitudinal variations within the detector for 1 mW input power. The modal power decays exponentially with light penetration depth due to local photon absorption. The optical power is highest near the front facet causing photo-generated carriers to pile up there. The increased band filling leads to a blue-shift of the absorption edge and a reduction of the signal absorption at 1545 nm wavelength. Therefore, the light penetrates deeper into the WPD and about 5% of the light power remains undetected (light reflection at the rear facet is neglected). The amount of undetected light grows with higher input power, leading to a non-linear detector response in Fig. 7.

The vertical profiles of electron density and conduction band edge are plotted in Fig. 9. The carrier pile-up in the quantum wells causes a partial screening of the electrostatic field flattening the conduction band edge profile. As a consequence, the carriers are less quickly removed from the quantum wells and the saturation effect is worsened. A higher reverse bias enhances the carrier removal from the quantum wells leading to a more linear response in Fig. 7. However, the strong saturation calculated for our quantum well detector at relatively low input power may require the use of Franz-Keldysh-type detectors in our wavelength converter. Such photon absorption by the reverse biased waveguide layer shows less saturation effects due to the missing carrier confinement.[1]

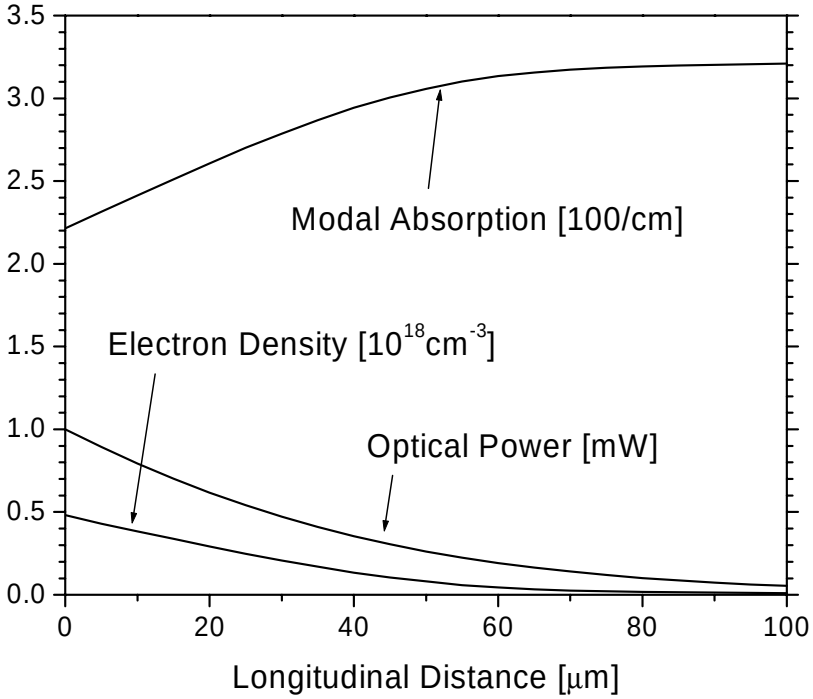

Fig. 8: Longitudinal variations of internal photodetector parameters.

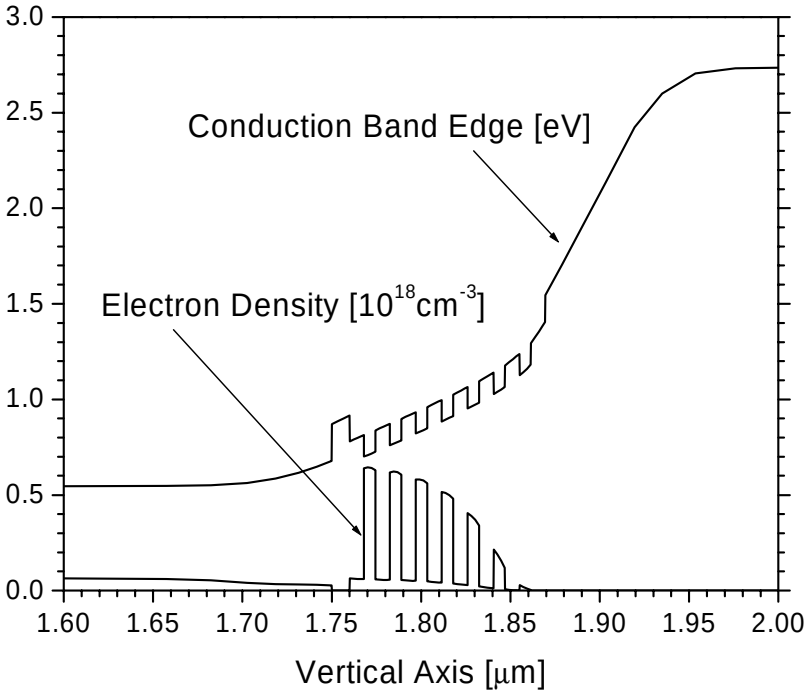

Fig. 9: Vertical variations of internal photodetector parameters.

6. SUMMARY

Advanced three-dimensional simulation of wavelength converter components including a realistic many-body model for gain and absorption is used to analyze quantum well saturation mechanisms that cause nonlinear signal transmission. Both amplifier and detector show a nonlinear response for input signal powers near 1 mW and above, which is mainly caused by quantum well carrier depletion and accumulation, respectively. The detector saturation is found to be most severe, due to the blue-shift of the absorption edge with increasing photo-generation of carriers.

ACKNOWLEDGMENT

This research project is sponsored by the Semiconductor Research Corporation (Award 2001-NJ-968) and by the Intel Corporation.

REFERENCES

[1] J. Hutchinson, J. Barton, M. Masanovic, M. Sysak, J. Henness, L. Johansson, D. Blumenthal, and L. A. Coldren, "Monolithically integrated InP-based tunable wavelength conversion." In: *Physics and Simulation of Optoelectronic Devices XII*, SPIE Proc. Vol. 5349, pp. 176-184, 2004.

[2] V. Jayaraman, A. Mathur, L. A. Coldren, and P. D. Dapkus, "Theory, design, and performance of extended tuning range in sampled grating DBR lasers," IEEE J. Quantum Electron., vol. 29, pp. 1824–1834, 1993.

[3] PICS3D by Crosslight Software, 2004.

[4] J. Piprek, N. Trenado, J. Hutchinson, J. Henness, and L. A. Coldren, "3D Simulation of an integrated wavelength converter." In: *Physics and Simulation of Optoelectronic Devices XII*, SPIE Proc. Vol. 5349, pp. 185-196, 2004.

[5] S.W. Koch, J. Hader, A. Tränhardt, and J.V. Moloney, "Gain and Absorption: Many-Body Effects," Chapter 1 in: *Optoelectronic Devices – Advanced Simulation and Analysis*, J. Piprek (ed.), Springer Verlag, New York, 2004.

[6] J. Piprek, S. Li, P. Mensz, and J. Hader, "Monolithic Wavelength Converter," Chapter 14 in: *Optoelectronic Devices – Advanced Simulation and Analysis*, J. Piprek (ed.), Springer Verlag, New York, 2004.